Generalized Parton Distributions in Hall A at Jefferson Lab

Carlos Muñoz Camacho

Institut de Physique Nucléaire, CNRS/IN2P3 (France)

Correlations in Partonic and Hadronic Interactions 2018
Yerevan (Armenia)

Outline

1. Introduction
2. Nucleon 3D-imaging & Generalized Parton Distributions (GPDs)
3. Deeply Virtual Compton Scattering (DVCS): $ep \to ep\gamma$
   - Results on both proton and neutron (preliminary)
4. Exclusive π^0 electroproduction (DVMP): $eN \to eN\pi^0$
   - Also: proton + neutron $\Rightarrow$ *flavor separation*
5. First (preliminary) results at 12 GeV and future plans
6. Summary

Deeply Virtual Compton Scattering (DVCS): $\gamma^* \, p \to \gamma \, p$

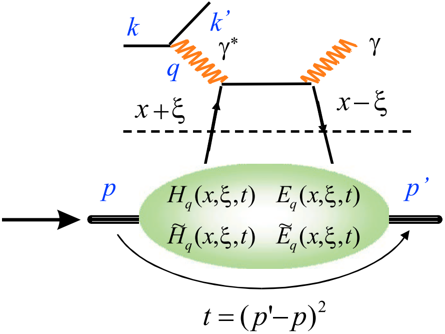

Handbag diagram

High Q^2
Perturbative QCD

Non-perturbative
GPDs

Bjorken limit :

$$\left. \begin{array}{rcl} Q^2 = & -q^2 \to & \infty \\ & \nu \to & \infty \end{array} \right\} \quad x_B = \frac{Q^2}{2M\nu} \text{ fixed}$$

DVCS experimentally: interference with Bethe-Heitler

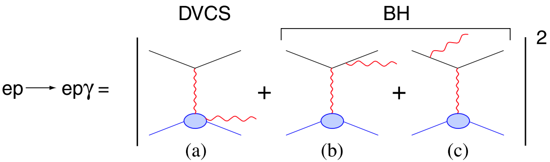

At leading order in $1/Q$ (leading twist) :

$$d^5\overrightarrow{\sigma} - d^5\overleftarrow{\sigma} = \Im m\left(T^{BH}\cdot T^{DVCS}\right)$$
$$d^5\overrightarrow{\sigma} + d^5\overleftarrow{\sigma} = |BH|^2 + \Re e\left(T^{BH}\cdot T^{DVCS}\right) + |DVCS|^2$$

$$\mathcal{T}^{DVCS} = \int_{-1}^{+1} dx \frac{H(x,\xi,t)}{x-\xi+i\epsilon} + \cdots =$$

$$\underbrace{\mathcal{P}\int_{-1}^{+1} dx \frac{H(x,\xi,t)}{x-\xi}}_{\text{Access in helicity-independent cross section}} - \underbrace{i\pi\, H(x=\xi,\xi,t)}_{\text{Access in helicity-dependent cross-section}} + \ldots$$

Leading twist GPDs

8 GPDs related to the different combination of quark/nucleon helicities

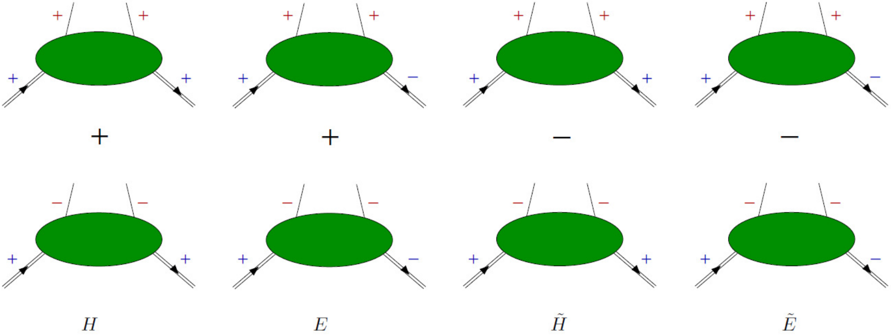

4 chiral-even GPDs: conserve the helicity of the quark

Access through DVCS (and DVMP)

Leading twist GPDs

8 GPDs related to the different combination of quark/nucleon helicities

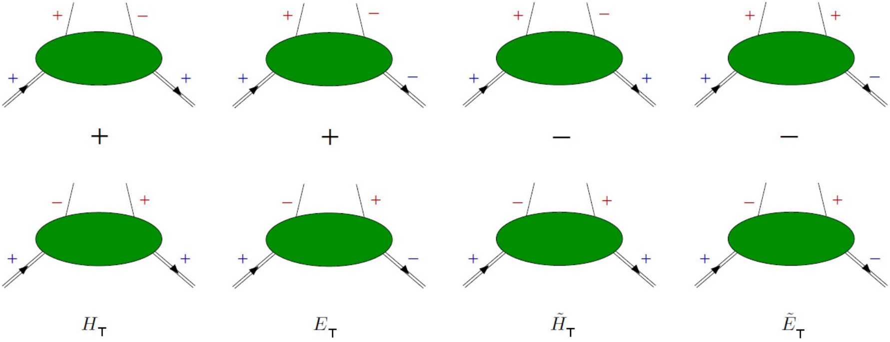

4 chiral-odd GPDs: flip helicity of the quark

"transversity GPDs"

Experimental access more complicated (π^0 electroproduction?)

Accessing different GDPs

Polarized beam, unpolarized target (BSA)

$$d\sigma_{LU} = \sin\phi \cdot \mathcal{I}m\{F_1\mathcal{H} + x_B(F_1+F_2)\tilde{\mathcal{H}} - kF_2\mathcal{E}\}d\phi$$

Unpolarized beam, longitudinal target (ITSA)

$$d\sigma_{UL} = \sin\phi \cdot \mathcal{I}m\{F_1\tilde{\mathcal{H}} + x_B(F_1+F_2)(\tilde{\mathcal{H}} + x_B/2\mathcal{E}) - x_B kF_2\tilde{\mathcal{E}} \ldots\}d\phi$$

Polarized beam, longitudinal target (BITSA)

$$d\sigma_{LL} = (A + B\cos\phi) \cdot \mathcal{R}e\{F_1\tilde{\mathcal{H}} + x_B(F_1+F_2)(\tilde{\mathcal{H}} + x_B/2\mathcal{E}) \ldots\}d\phi$$

Unpolarized beam, transverse target (tTSA)

$$d\sigma_{UT} = \cos\phi \cdot \mathcal{I}m\{k(F_2\mathcal{H} - F_1\mathcal{E}) + \ldots\}d\phi$$

Kinematic coverage

Kinematic complementarity between different facilities:

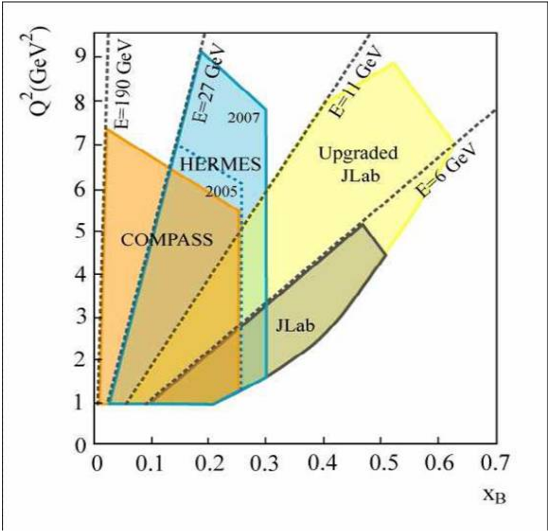

Experimental setup

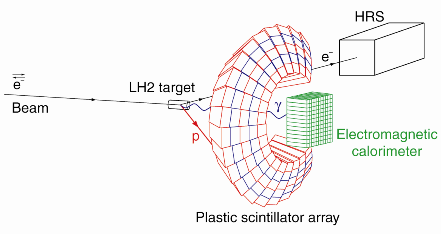

High Resolution Spectrometer

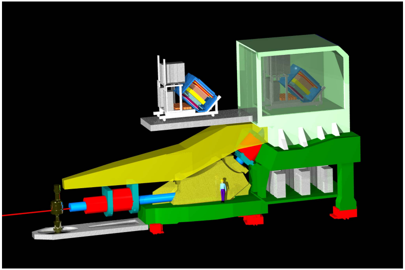

100-channel scintillator array

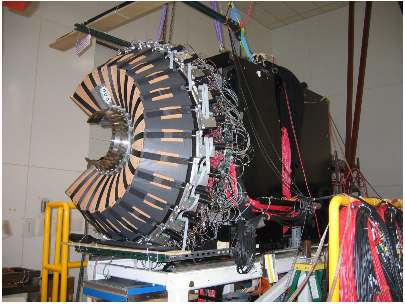

132-block PbF_2 electromagnetic calorimeter

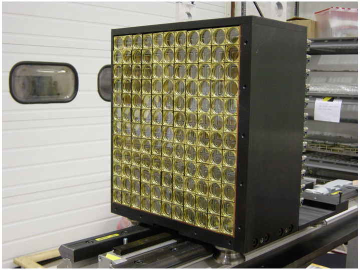

DVCS cross sections: azimuthal analysis

$Q^2 = 2.36$ GeV^2, $x_B = 0.37$, $-t = 0.32$ GeV^2

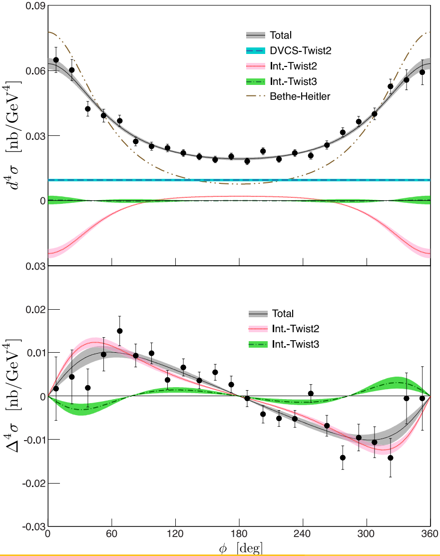

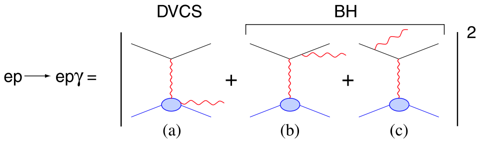

$$d^4\sigma = \mathcal{T}_{\mathsf{BH}}^2 + \mathcal{T}_{\mathsf{BH}}\mathcal{R}e(\mathcal{T}_{\mathsf{DVCS}}) + \mathcal{T}_{\mathsf{DVCS}}^2$$

$$\mathcal{R}e(\mathcal{T}_{\mathsf{DVCS}}) \sim c_0^{\mathcal{I}} + c_1^{\mathcal{I}}\cos\phi + c_2^{\mathcal{I}}\cos 2\phi$$

$$\mathcal{T}_{\mathsf{DVCS}}^2 \sim c_0^{\mathsf{DVCS}} + c_1^{\mathsf{DVCS}}\cos\phi$$

$$\Delta^4\sigma = \frac{d^4\overrightarrow{\sigma} - d^4\overleftarrow{\sigma}}{2} = \mathcal{I}m(\mathcal{T}_{\mathsf{DVCS}})$$

$$\mathcal{I}m(\mathcal{T}_{\mathsf{DVCS}}) \sim s_1^{\mathcal{I}}\sin\phi + s_2^{\mathcal{I}}\sin 2\phi$$

M. Defurne *et al.* Phys. Rev. C 92, 055202

DVCS cross sections: Q^2–dependance

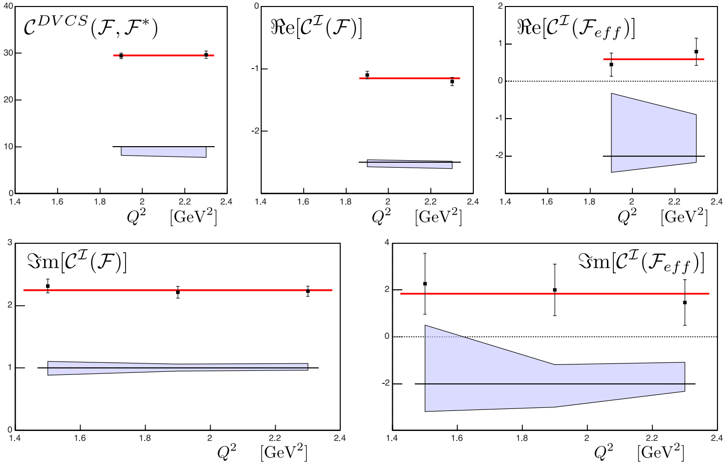

No Q^2-dependance within limited range $\Rightarrow$ leading twist dominance

DVCS cross sections: kinematical power corrections

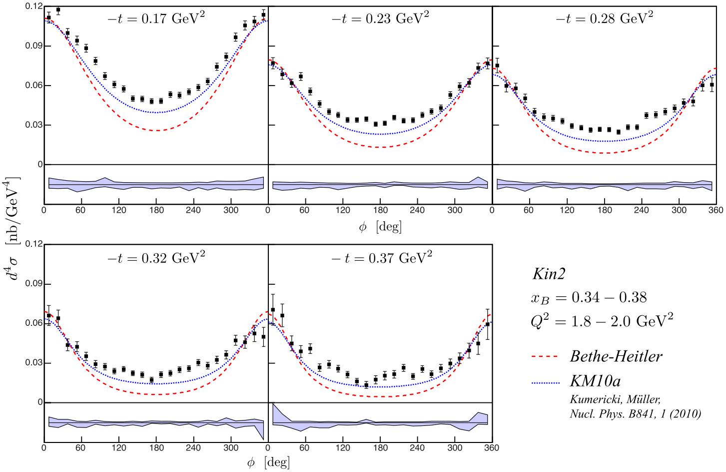

- KM10a: global fit to HERA x-sec & HERMES + CLAS spin asymmetries

Kumericki and Mueller (2010)

DVCS cross sections: kinematical power corrections

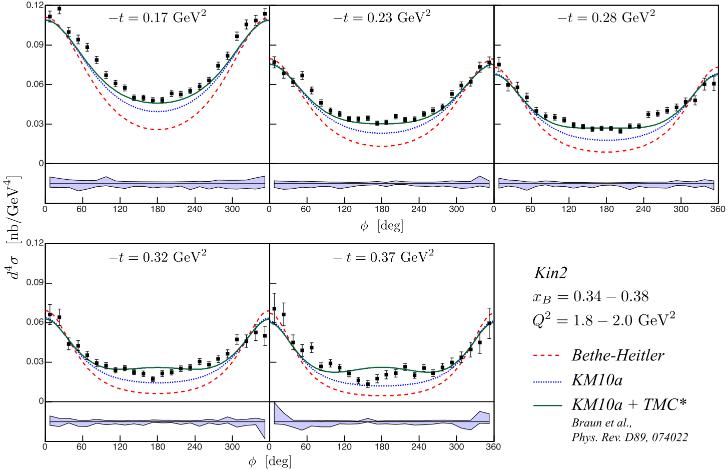

- KM10a: global fit to HERA x-sec & HERMES + CLAS spin asymmetries

  Kumericki and Mueller (2010)

- Target-mass corrections (TMC): $\sim \mathcal{O}(M^2/Q^2)$ and $\sim \mathcal{O}(t/Q^2)$

  Braun, Manashov, Mueller and Pirnay (2014)

Rosenbluth-like separation of the DVCS cross section

$$\sigma(ep \to ep\gamma) = \underbrace{|BH|^2}_{\text{Known to} \sim 1\%} + \underbrace{\mathcal{I}(BH \cdot DVCS)}_{\text{Linear combination of GPDs}} + \underbrace{|DVCS|^2}_{\text{Bilinear combination of GPDs}}$$

$$\mathcal{I} \propto 1/y^3 = (k/\nu)^3,$$
$$\left|\mathcal{T}^{DVCS}\right|^2 \propto 1/y^2 = (k/\nu)^2$$

BKM-2010 – at leading twist $\to$ 7 independent GPD terms:

$$\left\{\Re\mathrm{e}, \Im\mathrm{m}\left[\mathcal{C}^{\mathcal{I}}, \mathcal{C}^{\mathcal{I},V}, \mathcal{C}^{\mathcal{I},A}\right](\mathcal{F})\right\}, \quad \text{and} \quad \mathcal{C}^{DVCS}(\mathcal{F}, \mathcal{F}*).$$

φ-dependence provides 5 independent observables:

$$\sim 1, \sim \cos\varphi, \sim \sin\varphi, \sim \cos(2\varphi), \sim \sin(2\varphi)$$

The measurement of the cross section at two or more beam energies for exactly the same Q^2, x_B, t kinematics, provides the additional information in order to extract all leading twist observables independently.

DVCS process: leading twist ambiguity

- DVCS defines a preferred axis: light-cone axis
- At finite Q^2 and non-zero t, there is an ambiguity:
  1. Belitsky et al. ("BKM", 2002–2010): light-cone axis in plane (q,P)
  2. Braun et al. ("BMP", 2014): light-cone axis in plane (q,q')
     easi*er* to account for kin. corrections $\sim \mathcal{O}(M^2/Q^2)$, $\sim \mathcal{O}(t/Q^2)$

$$\left.\begin{array}{ll}\mathcal{F}_{++} = & \mathbb{F}_{++} + \frac{\chi}{2}\left[\mathbb{F}_{++} + \mathbb{F}_{-+}\right] - \chi_0 \mathbb{F}_{0+} \\ \mathcal{F}_{-+} = & \mathbb{F}_{-+} + \frac{\chi}{2}\left[\mathbb{F}_{++} + \mathbb{F}_{-+}\right] - \chi_0 \mathbb{F}_{0+} \\ \mathcal{F}_{0+} = & -(1+\chi)\mathbb{F}_{0+} + \chi_0\left[\mathbb{F}_{++} + \mathbb{F}_{-+}\right]\end{array}\right\} \xrightarrow[\mathbb{F}_{0+}=0]{\mathbb{F}_{-+}=0} \left\{\begin{array}{ll}\mathcal{F}_{++} & = (1+\frac{\chi}{2})\mathbb{F}_{++} \\ \mathcal{F}_{-+} & = \frac{\chi}{2}\mathbb{F}_{++} \\ \mathcal{F}_{0+} & = \chi_0 \mathbb{F}_{++}\end{array}\right.$$

(eg. $\chi_0 = 0.25$, $\chi = 0.06$ for $Q^2 = 2$ GeV^2, $x_B = 0.36$, $t = -0.24$ GeV^2)

E07-007: DVCS beam-energy dependence

- Cross section measured at 2 beam energies and constant Q^2, x_B, t

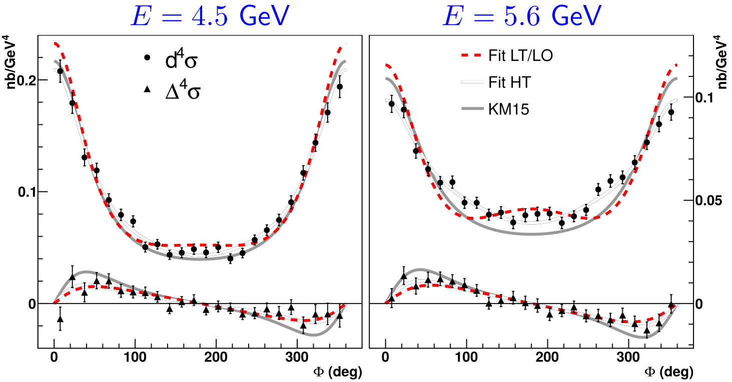

- Leading-twist and LO simultaneous fit of both beam energies (dashed line) does not reproduce the data

Light-cone axis in the (q,q') plane (Braun et al.): $\mathbb{H}_{++}$, $\widetilde{\mathbb{H}}_{++}$, $\mathbb{E}_{++}$, $\widetilde{\mathbb{E}}_{++}$

Beyond Leading Order (LO) and Leading Twist (LT)

Two fit-scenarios:

Light-cone axis in the (q,q') plane (Braun et al.)

LO/LT + HT

$\mathbb{H}_{++}$, $\widetilde{\mathbb{H}}_{++}$, $\mathbb{H}_{0+}$, $\widetilde{\mathbb{H}}_{0+}$

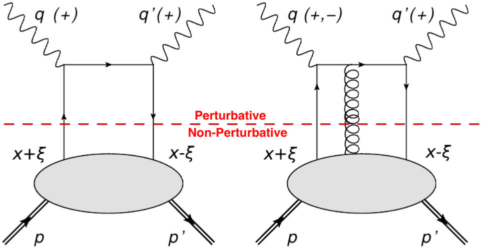

LO/LT + NLO

$\mathbb{H}_{++}$, $\widetilde{\mathbb{H}}_{++}$, $\mathbb{H}_{-+}$, $\widetilde{\mathbb{H}}_{-+}$

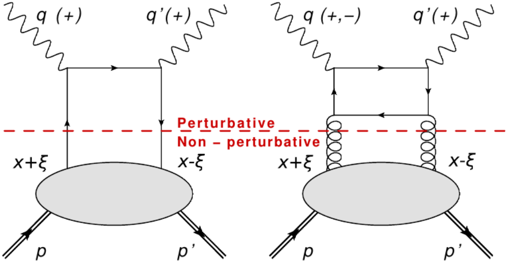

E07-007: DVCS beam-energy dependence

- Cross section measured at 2 beam energies and constant Q^2, x_B, t

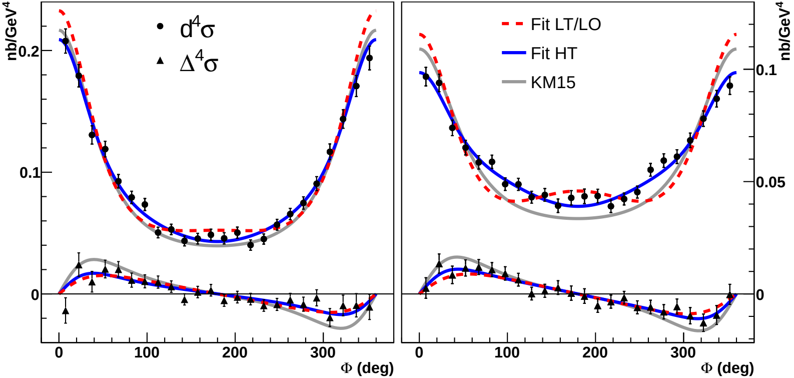

- Leading-twist and LO simultaneous fit of both beam energies (dashed line) does not reproduce the data
- Including either NLO or higher-twist effects (dark solid line) satisfactorily reproduce the angular dependence

DVCS^2 and $\mathcal{I}$(DVCS·BH) separation

DVCS^2 and $\mathcal{I}$(DVCS·BH) separated in NLO and higher-twist scenarios

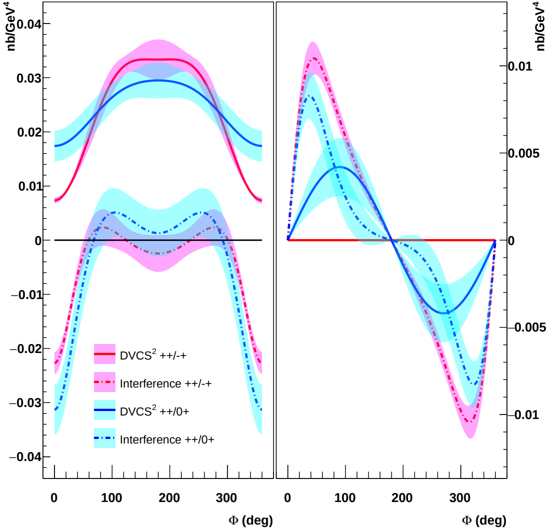

- DVCS^2 & $\mathcal{I}$ significantly different in each scenario
- Sizeable DVCS^2 contribution in the higher-twist scenario in the helicity-dependent cross section

Nature Commun. 8, 1408 (2017)

DVCS on the neutron: experiment E03-106 at JLab

LD_2 target ($F_2^n(t) \gg F_1^n(t)$!)

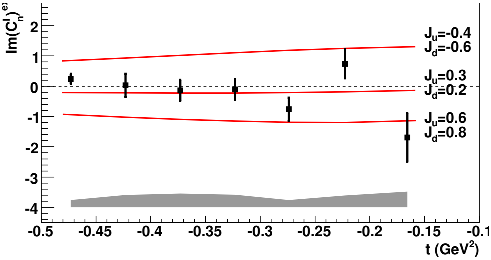

$$\sigma^{\rightarrow} - \sigma^{\leftarrow} = \Gamma(A \sin\varphi + \dots)$$

Charged particle veto
in front of scintillator array

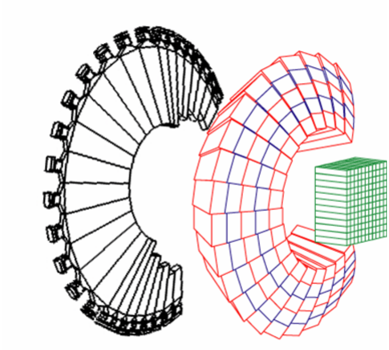

$$A = F_1(t)\mathcal{H} + \frac{x_B}{2-x_B}[F_1(t)+F_2(t)]\tilde{\mathcal{H}} - \underbrace{\frac{t}{4M^2} \cdot F_2(t) \cdot \mathcal{E}}_{\text{Main contribution for neutron}}$$

E08-025: DVCS off the neutron at different beam energies

- LD_2 as a target $(Q^2 = 1.75$ GeV^2, $x_B = 0.36)$
- Quasi-free p evts subtracted using the (normalized) data from E07-007
- Concurrent running: switching LD2/LD2 $\rightarrow$ minimize uncertainties

$$D(e, e\,\gamma)X - p(e, e\,\gamma)p = n(e, e\,\gamma)n + d(e, e\,\gamma)d$$

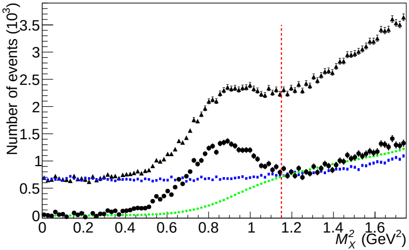

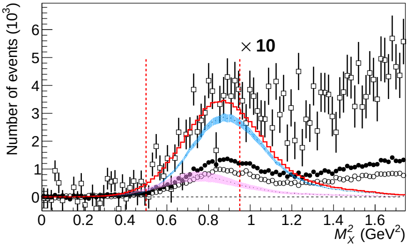

The average momentum transfer to the target is much larger than the np relative momentum, justifying this **impulse approximation**

π^0 electroproduction ($ep \to ep\pi^0$)

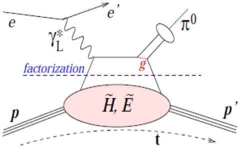

At leading twist:

$$\frac{d\sigma_L}{dt} = \frac{1}{2}\Gamma \sum_{h_N, h_{N'}} |\mathcal{M}^L(\lambda_M = 0, h'_N, h_N)|^2 \propto \frac{1}{Q^6} \qquad \sigma_T \propto \frac{1}{Q^8}$$

$$\mathcal{M}^L \propto \left[\int_0^1 dz \frac{\phi_\pi(z)}{z}\right] \int_{-1}^{1} dx \left[\frac{1}{x-\xi} + \frac{1}{x+\xi}\right] \times \left\{\Gamma_1 \widetilde{H}_{\pi^0} + \Gamma_2 \widetilde{E}_{\pi^0}\right\}$$

Different quark weights: flavor separation of GPDs

$$|\pi^0\rangle = \frac{1}{\sqrt{2}}\{|u\bar{u}\rangle - |d\bar{d}\rangle\} \qquad \widetilde{H}_{\pi^0} = \frac{1}{\sqrt{2}}\left\{\frac{2}{3}\widetilde{H}^u + \frac{1}{3}\widetilde{H}^d\right\}$$

$$|p\rangle = |uud\rangle \qquad H_{DVCS} = \frac{4}{9}H^u + \frac{1}{9}H^d$$

Exclusive π^0 electroproduction cross-sections – Hall A

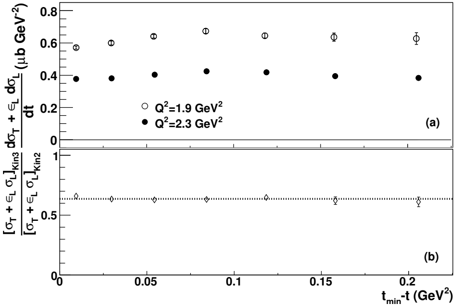

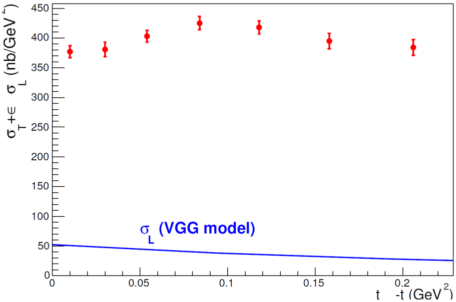

- $\sigma_T + \epsilon_L \sigma_L \sim Q^{-5}$
  (similar to $\sigma_T(ep \to ep\pi^+)$ measured in Hall C)
- GPDs predict $\sigma_L \sim Q^{-6}$
- σ_T likely to dominate at these Q^2,
  but L/T separation necessary ($\to$ new experiment. . .)

E. Fuchey et al., Phys. Rev. C83 (2011), 025125

Rosenbluth separation

$$\frac{d^4\sigma}{dQ^2 dx_B dt d\phi} = \frac{1}{2\pi}\Gamma(Q^2, x_B, E)\left[\frac{d\sigma_T}{dt} + \epsilon\frac{d\sigma_L}{dt} + \sqrt{2\epsilon(1+\epsilon)}\frac{d\sigma_{TL}}{dt}\cos\phi + \epsilon\frac{d\sigma_{TT}}{dt}\cos\right.$$

Kinematics

Setting	Q^2 (GeV^2)	x_B	E^{beam} (GeV)	ϵ
Kin1	1.50	0.36	3.355	0.52
			5.55	0.84
Kin2	1.75	0.36	4.455	0.65
			5.55	0.79
Kin3	2.00	0.36	4.455	0.53
			5.55	0.72

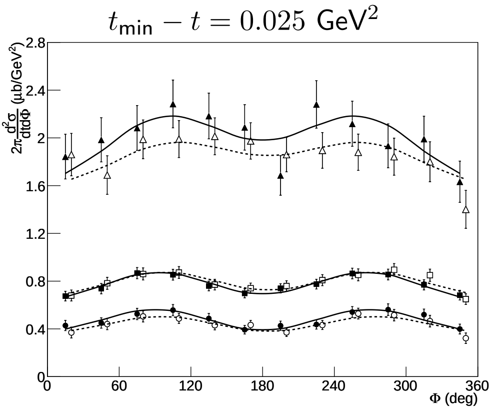

π^0 electroproduction and transversity GPDs

Modified handbag approach:

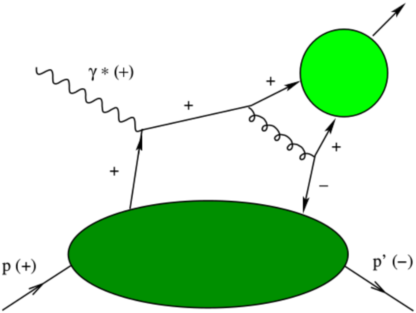

Divergencies regularized by $k_\perp$ of $q, \bar{q}$ + Sudakov suppression factor:

model of σ_T using transversity GPDs of the nucleon + twist-3 π DA

π^0 separated response functions

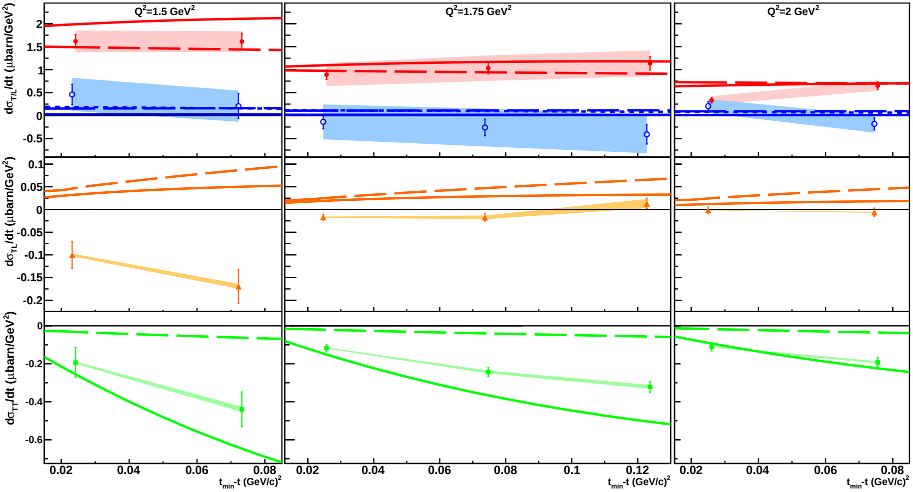

Goloskokov, Kroll (2011)

Goldstein, Hernandez, Liuti (2011)

Vanderhaeghen, Guichon, Guidal (1999)

E08-025: DVCS and π^0 off quasi-free neutrons

- LD$_2$ as a target
- Quasi-free p evts subtracted using the (normalized) data from E07-007
- Concurrent running: switching LD2/LD2 → minimize uncertainties

$$D(e, e\,\pi^0)X - p(e, e\,\pi^0)p = n(e, e\,\pi^0)n + d(e, e\,\pi^0)d$$

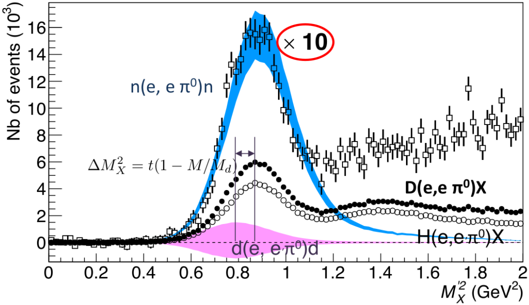

The average momentum transfer to the target is much larger than the np relative momentum, justifying this **impulse approximation**

π^0 electroproduction cross section off the neutron

- Cross section off coherent d found negligeable within uncertainties
- Very low E_{beam} dependence of the n cross section $\rightarrow$ dominance of σ_T

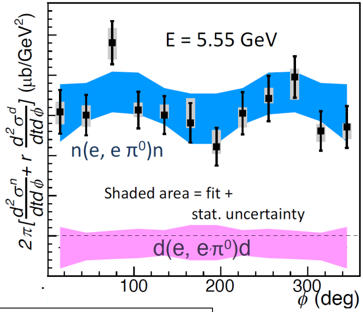

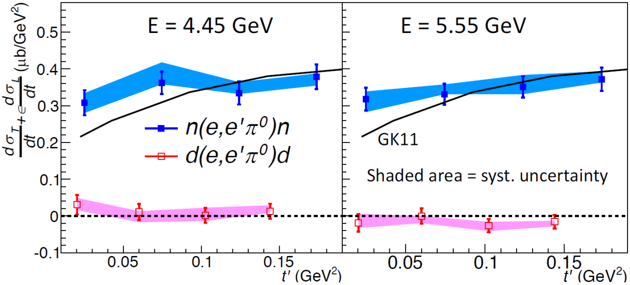

Separated π^0 cross section off the neutron

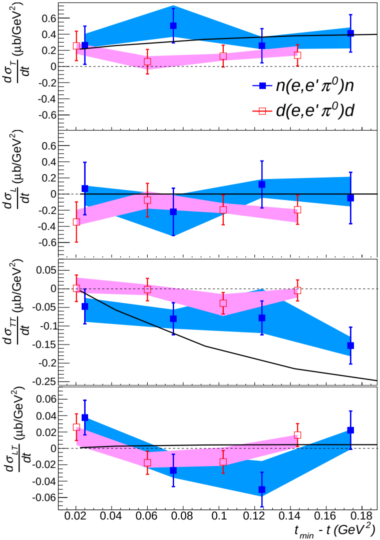

M. Mazouz et al, Phys.Rev.Lett. 118 (2017)

In the modified factorization approach (KG):

- $d\sigma_T \propto \left[\left(1-\xi^2\right) \left|\langle H_T \rangle\right|^2 - \frac{t'}{8M^2} \left|\langle \bar{E}_T \rangle\right|^2 \right]$
- $d\sigma_{TT} \propto \frac{t'}{8M^2} \left|\langle \bar{E}_T \rangle\right|^2$

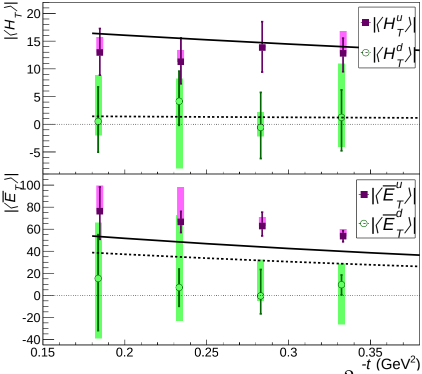

$$\left|\langle H_T^{p,n} \rangle\right|^2 = \frac{1}{2} \left| \frac{2}{3} \left\langle H_T^{u,d} \right\rangle + \frac{1}{3} \left\langle H_T^{d,u} \right\rangle \right|^2$$

E12-06-114: JLab Hall A at 11 GeV

JLab12 with 3, 4, 5 pass beam

(6.6, 8.8, 11.0 GeV beam energy)

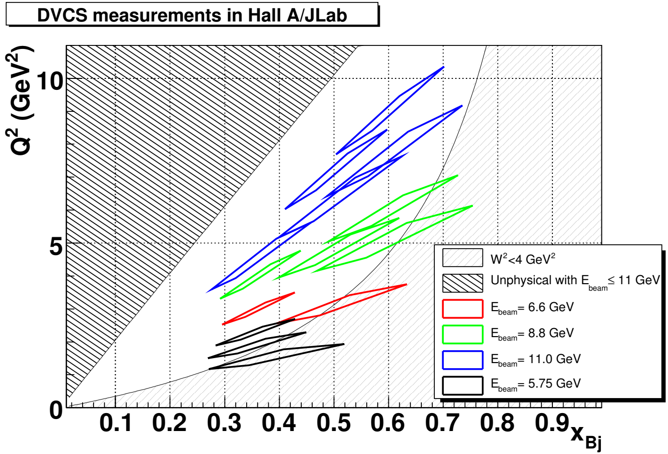

88 days

250k events/setting

1 year of operations in JLab/Hall A

Preliminary results

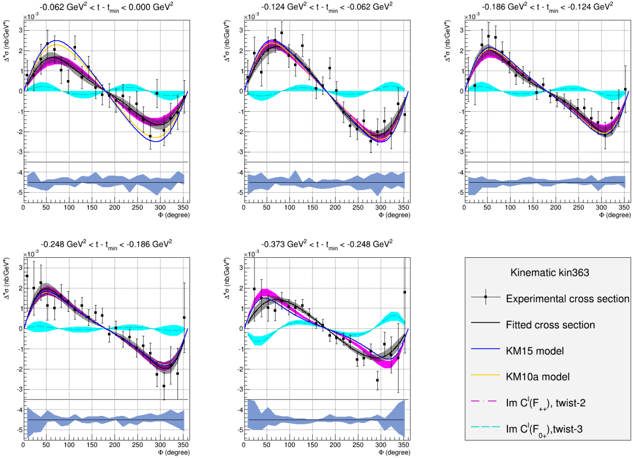

$Q^2 = 4.4\ GeV^2$
$x_B = 0.36$

25

F. Georges, SPIN 2018

E12-13-010: DVCS in Hall C

- HMS ($p < 7.3GeV$): scattered electron
- $PbWO_4$ calorimeter: γ/π^0 detection
- Sweeping magnet

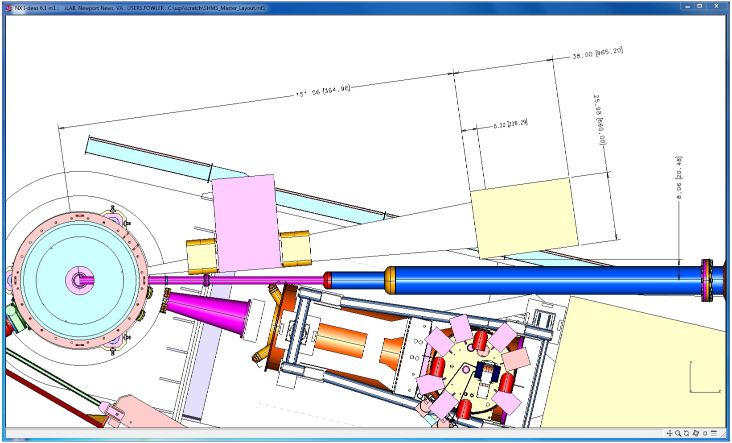

E12-13-010: beam energy separation in Hall C

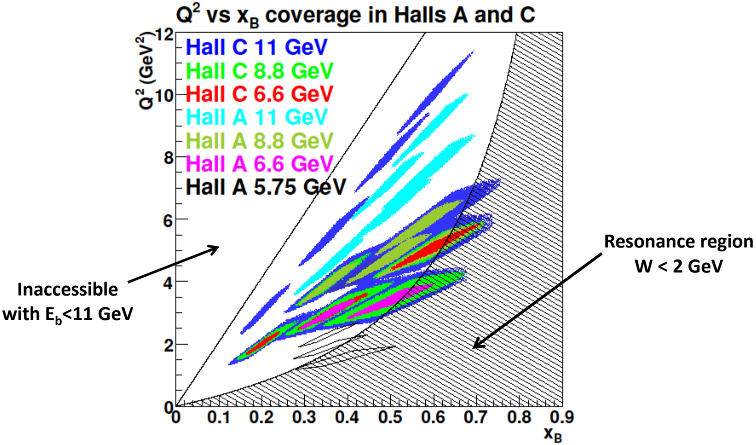

Approved by the PAC, possible running in $\gtrsim 2021$

Projections

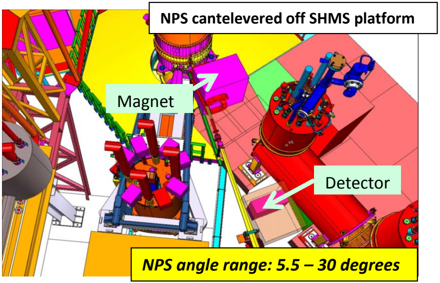

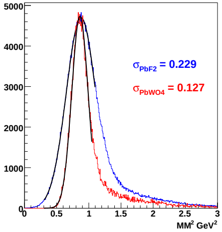

- $PbF_2 \rightarrow PbWO_4$
- Improved E resolution wrt Hall A

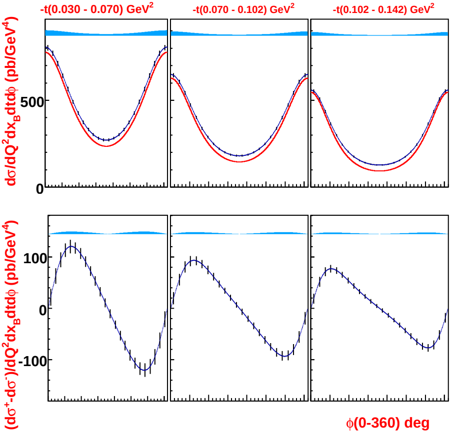

Summary

- Recent high precision DVCS cross sections from Hall A at JLab
- Need of higher twist and/or NLO contributions to fully describe the data (eg. in global GPD fits)
- First separation of DVCS^2 and BH-DVCS interference in the $eN \rightarrow e\gamma N$ cross section, off the proton and neutron
- L/T separation of π^0 electroproduction cross section off neutron: dominance of σ_T measured
- Flavor separation of transversity GPD convolutions within the modified factorization approach
- Approved program of experiments in Hall A and C to continue these high precision DVCS measurements at 12 GeV

Back-up